Interface adhesion assessment of composite-to-metal bonded joints under salt spray conditions using peel tests

Teixeira de Freitas, S.; Banea, M.D.; Budhe, S.; de Barros, S.

Important note
To cite this publication, please use the final published version (if applicable).
Please check the document version above.

Interface adhesion assessment of composite-to-metal bonded joints under salt spray conditions using peel tests

S. Teixeira de Freitas[a], M.D. Banea[b], S. Budhe[b], S. de Barros[b*]

[a]Delft University of Technology, Kluyverweg 1, 2629HS Delft,Netherlands

[b]Federal Center of Technological Education Celso Suckow da Fonseca-CEFET/RJ, Av. Maracanã, 229, 20271-110 Rio de Janeiro, RJ, Brazil

[*]Corresponding author: silvio.debarros@gmail.com (S. de Barros).

Abstract:

An experimental study has been carried out to assess the adhesion quality of composite-to-metal bonded joints under salt spray ageing conditions. The tests were performed according to the ASTM standard of floating roller peel tests with a new specimen layup. The layup and geometry of the specimen was defined in order to have the Carbon Fiber Reinforced Polymer (CFRP) and carbon steel as the rigid and flexible substrate, respectively. Specimens were exposed to salt spray (or salt fog) for 30 and 90 days. The results show that the adhesion performance (i.e. average peel load) of the joints progressively decreases with increasing the ageing time. The fracture surfaces of dry specimens (non-aged) exhibit a cohesive failure within the adhesive layer, which indicates a good adhesion between the CFRP-steel interfaces. Interface degradation is indicated by a drop in peel load and adhesive failure. The percentage of adhesive failure increases with aging times. Fracture surfaces of the adhesive failure exhibit deposition of NaCl crystal at the interface. Peel test successfully assessed the interface adhesion in aged and non-aged conditions, and can be used as a fast, easy and reliable test to study the long term durability in case of composite-metal bonded joints.

1. Introduction

There is an increasing need for reducing the weight in traditionally heavy loaded structures such as ships, offshore constructions and bridges, demanding the development of durable and lightweight solutions that can withstand heavy loads under extreme environmental conditions. Other sectors are facing similar drivers, such as aerospace and automotive, where 10% weight reduction can lead to 8% less fuel consumption [1, 2]. These have motivated the industry to engage on the quest to lightweight materials, capable to withstand high loads and deliver the guarantee of safety. The combination of metals and composites can reduce weight while preserving strength, leading to lighter and stronger structures. Within this type of structures, hybrid composite-to-metal joints are unavoidable. Adhesive bonding is the best suited joining technology for bonding dissimilar materials and for large stress-bearing areas (low stress concentrations), in comparison with traditional joining methods such as rivets and bolts [3-7]. However, the durability of bonded joints is one of the bottleneck that limits the use of adhesive bonding [8-10].

A number of environmental parameters such as moisture, temperature, thermal cycles, UV radiation, salt water, distilled water, humidity and so on are known to affect the durability of the bonded joints [11-15]. A review of the literature reveals that moisture, which can take the form of humidity or liquid water, is the most problematic substance when it comes to the durability of adhesive joints with fibre reinforced plastics (FRP) and metallic adherents [10-12]. Salt water is the worst to affect the joint performance, as metal get corrode also easily. As concerns the marine field, there has been an increasing demand for repairs using metallic-composite on floating offshore units such as Floating, Production, Storage and Offloading

2

(FPSO) [16]. Therefore, it is of prime importance to assess the interface adhesion between the metal-composite bonded joint in the presence of different environmental conditions. Rohem et al. [17] developed a new material and assessed the interface adhesion of steel-Glass Fiber Reinforced Polymers (GFRP) composite repair in marine applications and the joints successfully sustained the designed pressure without interface failure. Meniconi et al. [18] assessed the durability of adhesive joints for a metal-composite repair under salt spray ageing followed by the ultra violet radiation condition. They found that this environmental ageing was beneficial, as it caused almost 10% increase in critical shear stress of the interface. However, different combination of metal-composite joints need to be assessed for the interface adhesion, as each material have a different saturation limit [19]. For example, GFRP absorb more moisture content than the Carbon Fiber Reinforced Polymers (CFRP) [10]. Moisture can diffuse into resin matrix and cause plasticization, swelling, cracking, hydrolysis, and fibre/matrix debonding [13,20-21]. Moisture can also wick along fibre/matrix interface, leading to formation of micro-cracks, and thereby loss of integrity [22-25].

Considering the environmental durability of adhesive joints, there is limited research on the ageing effects on interface adhesion using a peel test. Single and double lap joints (SLJ and DLJ) and double cantilever beam (DCB) specimens are typically used to evaluate the environmental effect on the adhesion properties and strength [26-29]. Composite-composite and composite-metal bonded joints are well studied in the presence of different environment condition such as different humidity level, immersed in mineralized water, salt water at different temperature etc. [30-33]. Some authors combine SLJ with DCB or T-peel tests in order to evaluate the durability of bonded composite-to-aluminium joints, for example, against humidity, or the effect of different surface pre-treatment [34, 35]. Nevertheless, both studies were more focused on evaluating the effect on the mechanical properties rather than on evaluating the adhesion properties of the interfaces.

Interface adhesion is one of the most important parameters for assuring the integrity of bonded joints. Peel test is suitable to examine the interface adhesion properties, since the presence of mode I loading is the most severe for the interface, in comparison to mode II or mixed modes (SLJ and DLJ). Floating roller is an easy, fast and reliable type of peel test for metal bonding and is used for diverse objectives, including adhesives screening tests, effect of surface pre-treatments, bond durability, etc. [36-37]. Moreover, the asymmetry of substrates, unique in the floating roller peel test, allows to direct the evaluation to one interface, in opposition to, for example, DCB in which both interfaces are equally loaded. For metal bonding, the peel test is well documented and developed [38-40], but not the same case can be said for the composite-metal bonded joints. A simple and straight forward test coupon is needed to assess the adhesion of composite bonding and evaluates the interface of interest. Teixeira de Freitas et al. [41-42] successfully performed a peel test on composite-metal and composite-composite bonded joints.

However, limited research is available for evaluating the adhesion properties of composite-carbon steel joints under environment conditions. In this research, the influence of salt spray ageing on the adhesion properties of bonded composite-carbon steel joints is evaluated using the roller peel test.

2. Materials and specimens

2.1. Materials

To assess the interface adhesion between the bonded parts, peel test specimens were manufactured with carbon steel and CFRP substrates. The peel specimens consisted of

adhesively bonding the carbon steel as the flexible substrate with the CFRP as the rigid substrate (fig.1).
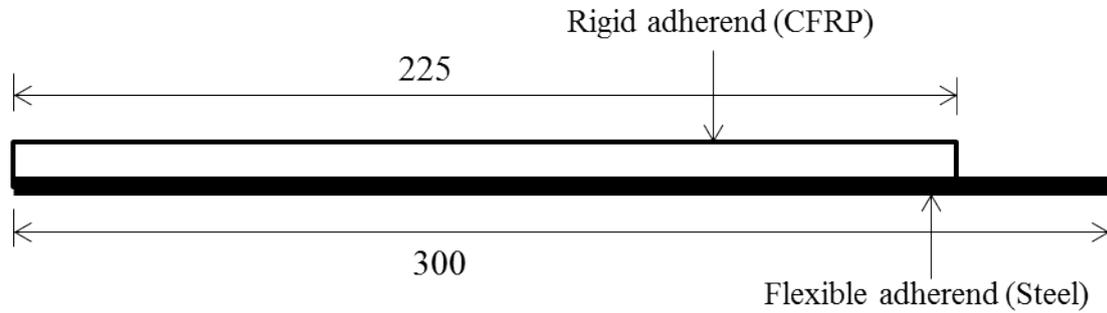
Figure 1. Peel sample with different peel length adherends (dimensions in mm).

The bi-component epoxy resin PIPEFIX[®] (NovatecLtd., Rio de Janeiro, Brazil) was used as an impregnation resin for the CFRP. A carbon steel plate (ASTM A36) with a thickness of 0.4 mm was used as a parent substrate. The bi-component epoxy adhesive NVT201E[®] (Novatec Ltd., Rio de Janeiro, Brazil) was used to join the dissimilar substrates. Carbon fiber dry woven with weight of 430 g/m² was taken for the composite preparation. Each ply was composed of two woven layers of carbon fiber [±45º]. One layer of glass fiber dry chopped strand mat (300 g/m²) was used to avoid direct contact between carbon fiber and steel plate. The material properties of composite laminates and adhesive were determined by conducting tensile tests according to ASTM D 3039 [43] and ASTM D638 [44] standard, respectively. The material properties of the composite laminate and adhesive are listed in table 1.

Table 1 Material properties of composite laminate and adhesive

Material Properties	Composite (Carbon biaxial ±45°)	Adhesive (NVT201E[®])
Tensile Strength [MPa]	651	50
Young's modulus [GPa]	46	2.30
Poisson Ratio	0.05	0.38

2.2.Sample preparation

The carbon steel plate was cleaned and passed through a grit blasting process with G-40 steel shot then it was degreased using acetone. The surface was analysed in a Taylor Hobson roughness Talyscan 150 (Leicester, UK) equipped with a 2 µm diameter styles probe. The scan speed was 1000 µm/s under temperature and humidity control (23°C and 60% RH). Figure 2 presents the 3D surface profile of the grit-blasted steel plate. The roughness parameters are presented in Table 1.
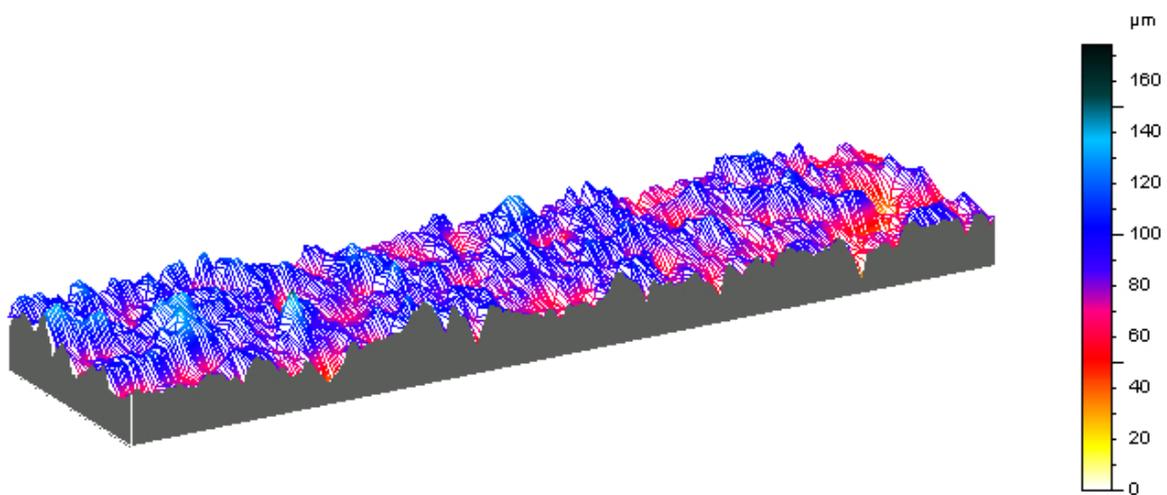
Figure 2. 3D surface profile of grit-blasted steel.

Table 1: Average surface roughness parameters (Ra – Arithmetic Mean Deviation of the roughness profile, Rt – Total Height of roughness profile, Sa – Arithmetic Mean Deviation of the Surface)

Ra (µm)	Rt (µm)	Sa (µm)
8.16	72.2	14.6

The epoxy adhesive was applied over the treated surface of steel plate prior to application of the glass fiber layer. Then the lamination process started by alternating application of

impregnation resin and carbon fiber fabric layers. Six ply of carbon fiber were used to produce the laminate with a final layup of $[\pm45°]_6$ and thickness of 3.55 ± 0.28 mm (average $\pm$ standard deviation). The curing time was 2 hours at room temperature.

Peel test specimen dimensions were based on the standard test method ASTM D 3167 [38] floating roller peel tests for metal bonding. Specimens were 25 mm in width and 300 mm long with a total thickness of 4.8 ± 0.3 mm (average$\pm$standard deviation) – see Fig.1.

3. Experimental methods

During testing, the flexible adherend (steel) is peeled off from the rigid adherend (CFRP). Standard floating roller peel tests (FRPT) were performed on both aged and non-aged specimens at room temperature (RT) conditions. Testing was carried out using an electro mechanic Zwick machine with maximum capacity of 20 kN, coupled with a load cell of 1 kN. The testing speed was 125 mm/min as per standard ASTM D3167 [45]. Figure 3 shows the tests set up of the peel test. In order to study the long term durability of the joint, the specimens were kept inside the salt spray cabinet (5% NaCl) for 30 days and 90 days. Three specimens were tested in each condition. During testing, load-displacement curves were recorded.
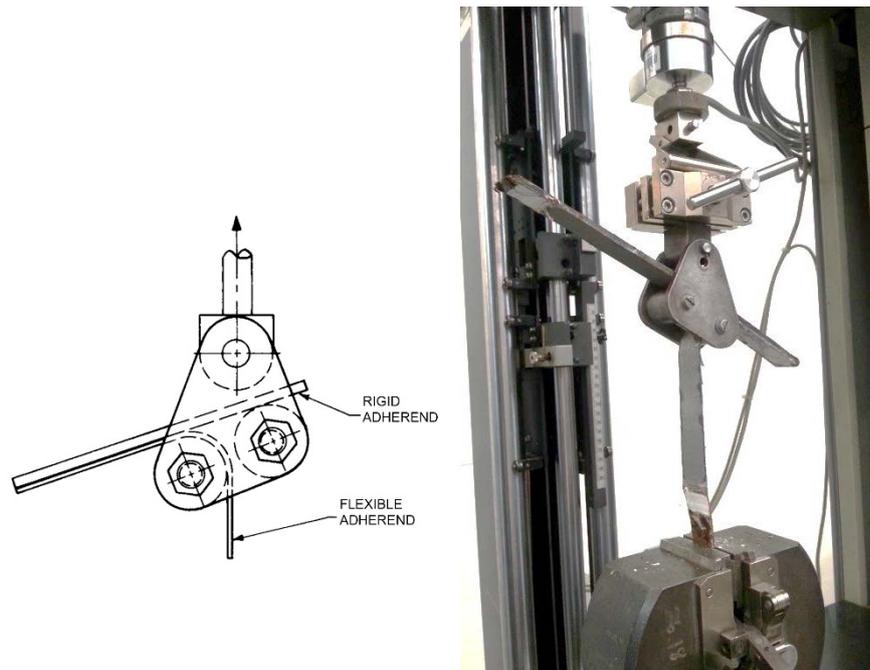
Figure 3. Floating roller peel test set up.

4. Results and Discussion

The average peel load and the failure mechanism of the specimens tested are given in Table 2. The average peel load values are shown as the average±standard deviation of the three specimens tested in each test condition. Two types of failure mechanism were observed: cohesive failure (CF) within the adhesive and adhesive failure (AF). The percentage area of failure modes is calculated based on the visual observation of specimen failure surface. The average failure peel load was determined along 150 mm of displacement, disregarding the first 20 mm. This procedure for determining failure peel load values is in accordance with ASTM standard D3167 [45].

Table2: Average peel loads and failure mechanisms

	F_{ave} (N/25 mm)	CF (%)	AF (%)
Non-aged	73.6±1.2	100	0
30 days in salt spray	65.3±3.0	95	5
90days in salt spray	56.5±13.4	60	40

After 30 days of exposure to salt spray (SS) the peel strength decreases in average by 11%. After 90 days in the SS, there is a quite significant reduction in peel load, in average about 23%, in comparison with non-aged specimens. The scatter in the peel strength increases also significantly after 90 days of exposure.
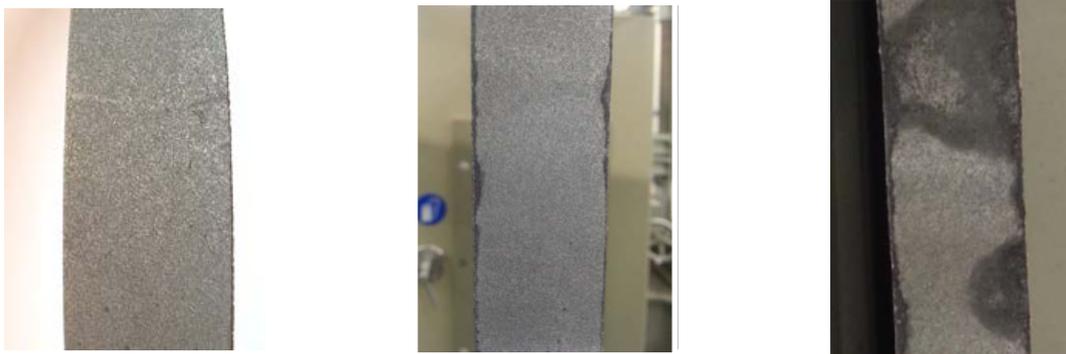
(a) non-aged   (b) 30 days in Salt Spray   (c) 90 days in Salt Spray

Figure 4. Examples of fracture surfaces of the flexible adherend (steel) after peel test.

Figure 4 shows a typical fracture surface of the steel substrate after testing. It can be seen that the cohesive failure was the dominant failure mode for the non-ageing condition – see Fig. 4(a). This indicates a good adhesion quality of the bonded joints. Cohesive failure was also the dominant failure mode after 30 days in salt spray condition, but small adhesive failure areas (less than 5%) were observed at the edges of the specimens – see Fig. 4(b). This implies

that after 30 days in SS the interface is marginally affected by the ingress of moisture. After 90 days of exposure, the adhesive failure areas increase significantly, which is also shown by the decrease in peel load. The pattern of the adhesive failure is also mainly at the edges of the specimens, but in some area crosses the complete width of the specimen, as shown in Fig 4 (c). The fracture surface of the ageing specimens shows that the moisture ingress is through the edges to the center of the specimen and it is not always affecting the complete adhesion surface. Increasing exposure times increases the moisture ingress and consequently adhesive failure areas and decreases the peel loads.

Figure 5 shows typical load-displacement curves measured during testing and the corresponding fracture surfaces of the flexible adherend (steel substrate).

The non-aged specimen presents a steady peel force along the complete displacement. Moreover, the peel load is within the range of 70N/25mm. The corresponding fracture surface is cohesive failure along the complete peel displacement.
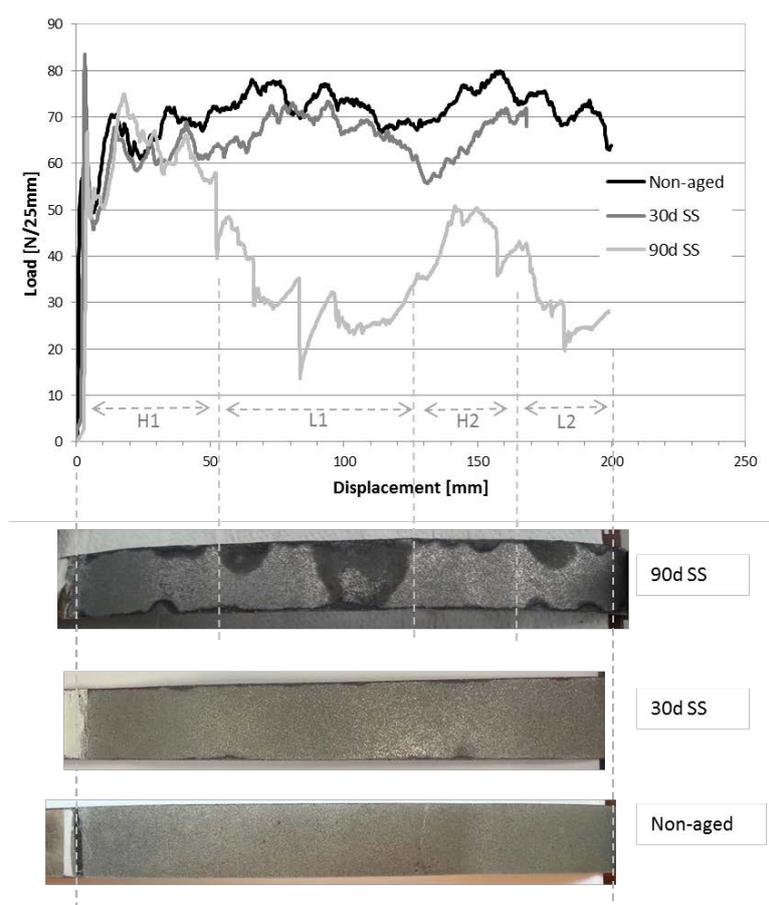
Figure 5. Load displacement curves non-aged, 30 days and 90 days aged on SS and the correspondent failure surface of the flexible adherends.

After 30 days in the SS cabinet, the peel strength decreases slightly. This corresponds well with the fracture surfaces since most of the failure observed is cohesive along the complete peel length.

The specimen aged for 90 days in the salt spray presents more unstable peel strength. The peel strength can be divided in four different areas along the displacement. In zone H1 – highlighted in the Figure 5, between 0 mm and +50 mm of displacement, the peel strength is very similar to the non-aged specimen, as is the failure surface which is mainly cohesive. In this area, the adhesive failures are located at the edges of the specimen. This is where the adhesion degradation starts, as this area in direct contact with the outside environment. This is followed by an area of lower peel strength – zone L1, between 50 mm and 125 mm, where

the peel strengths decrease significantly. This is justified by the change in failure mode from cohesive to adhesive failure, as can be confirmed in the corresponding fracture surface. In some areas the entire width of the cross section has been affected. This significantly decreases the peel strength, as a consequence of a loss of adhesion at the interface. Between 125 mm and 165 mm of the displacement, the peel strength increases again – area H2, but not reaching the initial peel strength. In this area the aging has progressed less from the edge to the center than in area L1 and therefore the peel strength is higher than in L1 but still significant adhesive failure is present. Finally, in zone L2, the area of adhesive failure increases due to further degradation at the interface, which results in a lower peel strength.

Although there is a consistent correlation between peel strength and failure modes, the areas of lower peel strength (i.e, adhesive failure) are not always at the same location for the three specimens aged for 90 days. The areas of moisture ingression are not always at the same location along the peel length. Literature shows that different factors such as surface roughness and/or interrupted deposition have an influence on the areas more prone to moisture ingression (and eventually corrosion rate) [46,47]. Therefore, both the manufacturing process (surface roughness of the steel) and salt spray condition (interrupted deposition of salt) can have an influence on the occurring time and place for interface debonding.

As shown, the peel strength is directly related with the failure modes, which is a result of the degradation of the interface due to ageing. Therefore, the peel strength can be used to assess the interface adhesion of steel-to-CFRP bonded joints under ageing. As stated in the literature [40-42], attention should be paid to only use peel strengths as a direct measure of adhesion performance if using comparable flexural stiffness of the flexible adherend. Different thickness or elastic modulus of the flexible adherend will result in changes in the peel strengths unrelated with the quality of the interface adhesion.

5. Fractographic analysis

In order to better understand the effect of the ageing phenomena in the adhesion performance, a detailed analysis of the fracture surfaces was performed using fractography.

The 90 days salt spray aged specimen presented in Figure 4 (c) was selected to conduct a fractographic analysis of the different failure surfaces present along the peel length. The analysis consisted in, firstly, visually observe the exposed fracture surfaces, secondly, select areas of interest using optical microscopy and finally characterize the selected areas using Scanning Electron Microscope (SEM).

Table 3 shows pictures taken from an area at one of the edges of the specimen where moisture ingress can be visually observed. The optical microscopic images (top) show the typical failure modes: adhesive failure (AF) and cohesive failure (CF), and a "flower-like" pattern of the moisture ingress from the edge to the center of the specimen's width. SEM pictures were taken from three spots: (1) at the very edge of the specimen (AF), (2) farther from the edge, but still in the degraded area (AF) and (3) a non-degraded area with cohesive failure. SEM pictures were taken both at the steel side and correspondent CFRP side (2nd and 3rd row, respectively).

The fracture surfaces at the edge of the specimen –spot (1), 1st column, present a very rough fracture surface and particularly at the steel side, the surface texture suggest a deposition of salt crystals. At spot (2) – 2nd column, one can observe the same rough surface as in spot (1) with a transition to a smoother surface at the right bottom corner of both pictures (flexible and rigid adherends). Finally, on the cohesive failure area – spot (3), 3rd column, on the flexible adherend (steel side), there are areas of smooth surfaces and areas of rough surfaces. The rougher surfaces include also air voids which suggest that, adhesive is present on those areas. The smoother surfaces can indicate an area of the interface with steel. On the rigid

adherend side the air voids can also be observed on the adhesive. Smoother and rougher surfaces can also be identified.

Table 3 – SEM pictures of typical fracture surfaces of the peel specimens.

Flexible adherend (x1)	(1)	(2)	(3)
Flexible ad. (Steel)	(SEMx500)	(SEM x500)[2]	(SEM x150)[1]
Rigid ad.(CFRP/Adhesive)	(SEM x500)	(SEM x500)	(SEM x150)
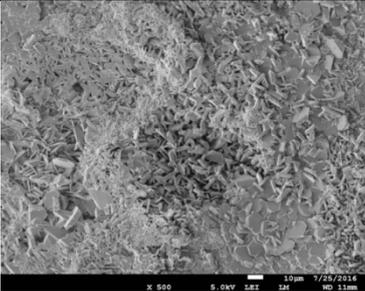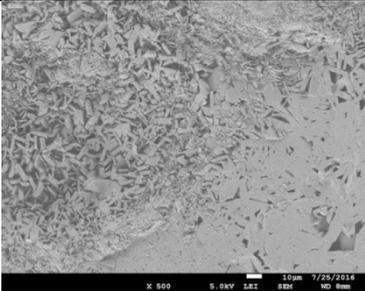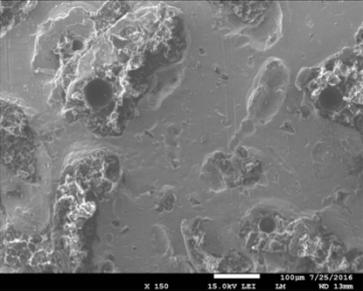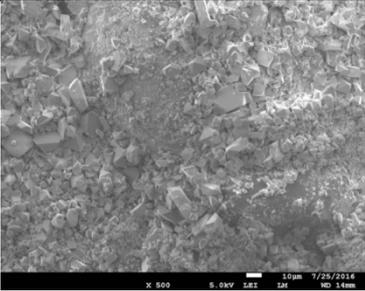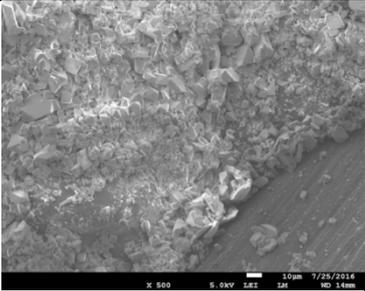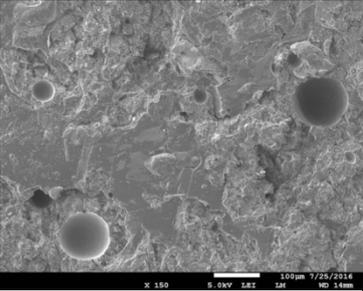
[1]shown also in Figure 6; chemical characterization in Figure 7(a)

[2]chemical characterization in Figure 7(b)

In order to have a better understanding of which components are present in the fracture surfaces, a chemical characterization of some images has been performed by using Energy-Dispersive Spectroscopy (EDS), available in the SEM equipment.

Figure 6 compares the SEM picture with the EDS scale grey using back scatter. The image corresponds to a spot (3) steel side of Table 3. The white areas in Figure 6 (b) are predominantly metal and the black areas are carbon, meaning adhesive. This picture shows that, in the cohesive failure zone, the crack grows very close to the flexible adherend, in some areas within the adhesive (black areas in Fig. 6(b)) but also at the interface (white areas in Fig 6 (b)).
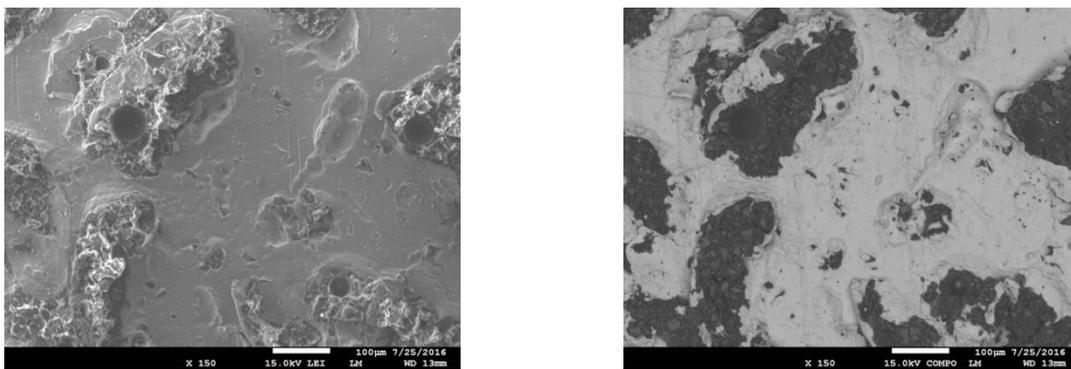
(a) SEM   (b) EDS

Figure 6. Typical SEM cohesive failure fracture surface (a) and corresponding EDS grey scale image (b).

Figure 7 compares the EDS spectrum of a typical cohesive failure – Fig. 7(a) and adhesive failure – Fig 7(b). The results of this spectrum suggest the presence of Chloride (and Sodium) in the adhesive failure fracture surfaces Fig. 7(b), which is not present in the cohesive surfaces (Fig 7(a)). This confirms that the crystals shapes observed in the SEM pictures of adhesive failure (spot 1 and 2 in Table 3) are NaCl crystals which were typically present at the adhesive failure areas due to ingress of salt within the interface.

15
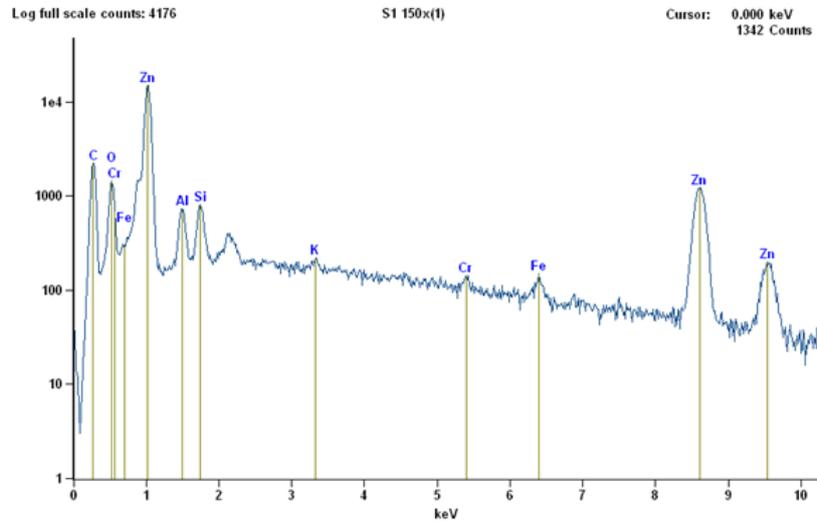
(a)
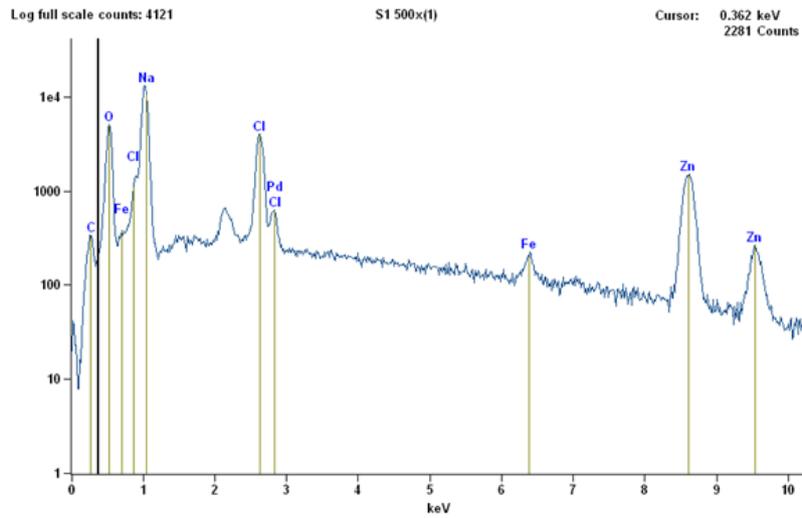
(b)

Figure 7. EDS spectrum of typical (a) CF and (b) AF.

6. Conclusions

Floating roller peel tests were performed in order to assess the interface degradation under salt spray conditions of composite-steel adhesively bonded joints. The standard peel tests

were adapted to tests hybrid structures (metal-composite). From the analysis of the results and of the fracture surfaces, the following conclusions can be drawn:

- There is limited reduction in the adhesion performance (i.e. peel strength) after 30 days of exposure to salt spray, but for longer exposure periods (90 days) a notable change in peel strength with respect to the non-aged specimen is observed (about 23% decrease).

- The non-aged specimens showed 100% cohesive failure, while aged specimens showed both cohesive and adhesive failure. The % area of cohesive failure depends on the exposed time of specimen to salt spray. Increasing the exposure time (90 days in salt spray) increases the adhesive failure, which indicates an increase in interface degradation.

- The fracture surface of the aged specimens indicates that the moisture ingress is from the edges and towards the centre of the specimen in a "flower-like" pattern. The area affected by moisture ingress depends on the exposed time of specimen to salt spray.

- Moisture affected areas showed a rough fracture surface, particularly at the steel side (crystal shape suggests a deposition of salt crystal). EDS analysis of those surfaces showed the presence of chloride and sodium,which confirms the deposition of NaCl crystals as a typical feature of adhesive failure due to degradation and ingress of salt within the interface.

- Cohesive failure occurs very close to the interface between the steel and the adhesive, and a closer look to the fracture surfaces reveal some areas of interface failure.

- Peel test has successfully assessed the interface adhesion in aged and non-aged conditions, and can be used as a fast, easy and reliable test to study the long term durability of composite-metal bonded joints.

References

[1] Das S. Life Cycle Assessment of Carbon Fiber-Reinforced Polymer Composites. The Int J LCA 2011; 16:268-282.

[2] Cheah LW. Cars on a Diet: The Material and Energy Impacts of Passenger Vehicle Weight Reduction in the U.S. PhD Thesis, The Engineering Systems Division, MIT USA 2010.

[3] Banea MD, da Silva LFM. Adhesively bonded joints in composite materials-An Overview. Proc I Mech Part L: J Mater Des Appl 2009; 223(1):1-18.

[4] Arenas JM, Alía C, Narbón JJ, Ocaña R, González C. Considerations for the industrial application of structural adhesive joints in the aluminium-composite material bonding. Compos Part B: Eng 2013;44:417-423.

[5] Rudawska A. Adhesive joint strength of hybrid assemblies: Titanium sheet-composites and aluminium sheet-composites-Experimental and numerical verification. Int J Adhes Adhes 2010;30:574-582.

[6] de Freitas ST, Sinke J. Failure analysis of adhesively-bonded skin-to-stiffener joints: Metal–metal vs. composite–metal. Eng Fail Anal 2015;56:2-13.

[7] Budhe S, Banea MD, de Barros S, da Silva LFM.An updated review of adhesively bonded joints in composite materials. Int J Adhes Adhes 2017;17:30-42.

[8] Wang. C, Huang YD, Xv HY, Liu WB. The durability of adhesive/carbon-carbon composites joints in salt water. 2004;246:471:477.

[9] Baldan A. Adhesion phenomena in bonded joints. Int J Adhes Adhes 2012;38:95-116.

[10] Heshmati M, Haghani R, Al-Emrani M. Effects of moisture on the long-term performance of adhesively bonded FRP/steel joints used in bridges. Compos Part B-Eng. 2016;92:447-62.

[11] Karbhari VM, Chin JW, Hunston D, Benmokrane B, Juska T, Morgan R, Lesko JJ, Sorathia U, Reynaud D. Durability Gap analysis for fiber-reinforced polymer composites in civil infrastructure. J Compos Constr 2003;7:238:247.

[12] Karbhari VM. Durability of composites for civil structural applications. Woodhead Pub.2007.

[13] Karbhari VM. Rehabilitation of metallic civil infrastructure using fiber reinforced polymer (FRP) composites: a materials and systems overview at the adhesive bond level. Woodhead Pub.2014.

[14] Boer P, Holliday L, Kang TH-K. Independent environmental effects on durability of fiber-reinforced polymer wraps in civil applications: a review. Constr Build Mater 2013;48:360-370.

[15] Boer P, Holliday L, Kang THK. Interaction of environmental factors on fiber reinforced polymer composites and their inspection and maintenance: a review. Constr Build Mater2014;50:209-218.

[16] de Barros S, Banea MD, Budhe S, de Siqueira CER, Lobão BSP, Souza LFG. Experimental analysis of metal-composite repair of floating offshore units (FPSO). J Adhes 2017;93:147-158.

[17] Rohem NRF, Pacheco LJ, Budhe S, Banea MD, Sampaio EM, de Barros S. Development and qualification of a new polymeric matrix laminated composite for pipe repair. Compos Struct 2016;152:737-745.

[18] Meniconi LCM, Lana LDM, Morikawa SRK. Experimental fatigue and aging evaluation of the composite patch repair of a metallic ship hull. Appl Adhes Sci 2014, 2:27

[19] Kohan MI. Nylon Plastics Handbook (Hanser-Gardner Publications, Cincinnati, OH, 1995.

[20] Chin JW, Nguyen T, Aouadl K. Effects of environmental exposure on fiber reinforced plastic (FRP) materials used in construction. J Compos Technol Res 1997;19:205-213.

[21] Zhou J, Lucas JP. Hygrothermal effects of epoxy resin. Part I: the nature of water in epoxy. Polymer 1999;40:5505-5512.

[22] Weitsman YJ. Anomalous fluid sorption in polymeric composites and its relation to fluid-induced damage. Compos Part A Appl Sci Manuf 2006;37: 617-623.

[23] Karbhari VM, Ghosh K. Comparative durability evaluation of ambient temperature cured externally bonded CFRP and GFRP composite systems for repair of bridges. Compos Part A Appl Sci Manuf 2009;40:1353-1363.

[24] Nishizaki I, Meiarashi S. Long-term deterioration of GFRP in water and moist environment. J Compos Constr 2002;6:21-27.

[25] Pierron F, Poirette Y, Vautrin A. A novel procedure for identification of 3D moisture diffusion parameters on thick composites: theory, validation and experimental results. J Compos Mater 2002;36:2219-2243.

[26] Owens J, Lee-Sullivan P. Stiffness behaviour due to fracture in adhesively bonded composite-to-aluminum joints II. Experimental. Int J Adhes Adhes 2000;20(1):47-58.

[27] Giannis S, Hansen K. 25th Technical Conference of the American Society for Composites and 14th US-Japan Conference on Composite Materials (Dayton, Ohio, USA, 2010.

[28] Fernandes RL, de Moura M, Moreira RDF. Effect of moisture on pure mode I and II fracture behaviour of composite bonded joints. Int J Adhes Adhes 2016;68:30-38.

20

[29] Sugiman S, Crocombe AD. The static and fatigue responses of aged metal laminate doublers joints under tension loading. J Adhes Sci Technol. 2016;30(3):313-327.

[30] Han X, Crocombe AD, Anwar SNR, Hu P. The strength prediction of adhesive single lap joints exposed to long term loading in a hostile environment. Int J Adhes Adhes 2014;55:1-11.

[31] Liu SF, Cheng XQ, Zhang Q, Zhang J, Bao JW, Guo X. An investigation of hygrothermal effects on adhesive materials and double lap shear joints of CFRP composite laminates. Compos Part B-Eng. 2016;91:431-440.

[32] Papanicolaou GC, Charitidis P, Mouzakis DE, Karachalios E, Jiga G, Portan DV. Experimental and numerical investigation of balanced Boron/Epoxy single lap joints subjected to salt spray aging. Int J Adhes Adhes 2016;68:9-18.

[33] Zhang F, Wang HP, Hicks C, Yang X, Carlson BE, Zhou Q. Experimental study of initial strengths and hygrothermal degradation of adhesive joints between thin aluminum and steel substrates. Int J Adhes Adhes 2013;43:14-25.

[34] Halliday ST, Banks WM, Pethrick RA. Influence of humidity on the durability of adhesively bonded aluminium composite structures. Proc Inst Mech Eng Part L: J Mater Des Appl 1999;213:27-35.

[35] Rhee K, Yang J. A study on the peel and shear strength of aluminum/CFRP composites surface-treated by plasma and ion assisted reaction method. Compos Sci Technol 2003;63:33-40.

[36] Hart-Smith LJ. A peel-type durability test coupon to assess interfaces in bonded, co-bonded, and co-cured composite structures, Int J Adhes Adhes 1999;19:181-191.

[37] Sargent JP. Durability studies for aerospace applications using peel and wedge tests. Int J Adhes Adhes 2005;25:247-256.

[38] Kawashita LF, Kinloch AJ, Moore DR, Williams JG. A critical investigation of the use of a mandrel peel method for the determination of adhesive fracture toughness of metal-polymer laminates. Eng Fract Mech 2006;73:2304-2323.

[39] Kawashita LF, Moore DR, Williams JG. Comparison of Peel Tests for Metal–Polymer Laminates for Aerospace Applications. J Adhes 2005;81:561-586.

[40] Kawashita LF, Moore DR, Williams JG. The development of a mandrel peel test for the measurement of adhesive fracture toughness of epoxy–metal laminates. J Adhes 2004;80:147-167.

[41] de Freitas ST, Sinke J. Test method to assess interface adhesion in composite bonding. Appl Adhes Sci 2015;3-9.

[42] de Freitas ST, Sinke J. Adhesion properties of composite-to-aluminium joints using peel tests. J adhes 2014;90(5-6):511-525.

[43] ASTM D3039 (2006) Standard test method for tensile properties of polymer matrix composite materials.

[44] ASTM D 638 (2002) Standard test method for tensile properties of plastics.

[45] ASTM-D3167 (2010) Standard Test Method for Floating Roller Peel Resistance of Adhesive.

[46] Oliveira JC, Cavaleiro A, Brett CMA. Influence of sputtering conditions on corrosion of sputtered W–Ti–N thin film hard coatings: salt spray tests and image analysis. Corros Sci 2000;42(11):1881-1895.

[47] Zhang J,Zhao X, Zuo Y, Xiong J. The bonding strength and corrosion resistance of aluminum alloy by anodizing treatment in a phosphoric acid modified boric acid/sulfuric acid bath. Surf Coat Tech 2008;202(14):3149-3156.